A Comparison of Tangent Screen, Goldmann, and Humphrey Perimetry in the Detection and Localization of Occipital Lesions

Agnes M.F. Wong, MD, James A. Sharpe, MD

Objective: To compare manual kinetic perimetry with tangent screen and Goldmann techniques and automated static perimetry with the Humphrey Field Analyzer in the detection and localization of occipital lobe lesions.

Design: Prospective consecutive comparative case series.

Participants: Twelve patients with well-defined occipital lobe infarcts on magnetic resonance (MR) imaging were studied.

Main Outcome Measures: The patients were tested by tangent screen, Goldmann, and Humphrey perimetry (central 30-2 threshold program). The three visual fields were compared and correlated with MR images.

Results: All three perimetric techniques *detected* the presence of postchiasmal lesions. However, *localization* of lesions differed with perimetric technique. Visual fields obtained from tangent screen and Goldmann perimetry were similar and corresponded well with the location of lesions on MR images in all 12 patients. Humphrey perimetry inaccurately localized the lesion to the proximal part of the postchiasmal pathway by revealing incongruous fields in two patients, failed to detect sparing of the posterior occipital cortex or occipital pole in four patients, and estimated a larger extent of damage in one patient when compared with MR images and manual perimetry.

Conclusions: All three perimetric techniques are satisfactory screening tests to detect occipital lesions. However, tangent screen and Goldmann perimetry provide information about the location and extent of lesions that is more consistent with prevailing knowledge of the effects of the lesion in the postgeniculate visual pathway.
Ophthalmology 2000;107:527–544 © 2000 by the American Academy of Ophthalmology.

Automated static perimetry is extensively used to identify visual field abnormalities in neurologic diseases. It has been demonstrated to be comparable to manual kinetic perimetry in *detecting* visual field loss in glaucoma[1–3] and neurologic diseases.[4,5] However, the accuracy of different perimetric techniques in *localizing* lesions in neurologic diseases has not been determined. Because the site and extent of lesions can be identified by magnetic resonance imaging (MRI) and because occipital lobe lesions cause well-recognized retinotopic patterns of visual field loss, the precision of perimetric techniques can be determined by correlating visual field defects with MR images of occipital lobe lesions. In contrast, retinotopic correlates of lesions of the optic nerve, chiasm, or optic tract are not well defined by imaging. In this study, we systematically evaluated and compared the accuracy of manual kinetic (tangent screen and the Goldmann perimeter) and automated static perimetry (Humphrey Field Analyzer) in detecting and localizing lesions by correlating them with MR images in patients with occipital lobe infarcts.

Materials and Methods

Consecutive patients with homonymous hemianopia on screening with Humphrey perimetry were recruited into the study from the Neuro-ophthalmology Unit at The Toronto Hospital. Serial axial and sagittal T1-weighted (TR, 516–517 msec; TE, 8–11 msec) and T2-weighted (TR, 2200–4383 msec; TE, 80–95 msec, two separate acquisitions) MR images were obtained (slice thickness, 5 mm), with the Signa 1.5 Tesla system (version 5.4.2/General Electric Medical Systems, Milwaukee, WI). Patients with well-defined occipital infarcts on MRI were included in the study.

Detailed visual field examinations were performed with a tangent screen, the Goldmann perimeter, and the Humphrey Field Analyzer. They were performed within 1 month of one another and within 3 months of imaging. Tangent screen (Bjerrum) kinetic

Received: April 23, 1999.
Revision accepted: October 14, 1999. Manuscript no. 99196.

From the Division of Neurology and Department of Ophthalmology, University Health Network–Toronto Western Hospital, and the University of Toronto, Toronto, Ontario, Canada.

Supported by Medical Research Council of Canada Grant MA15362 and by the E. A. Baker Foundation, Canadian National Institute for the Blind.

The authors have no commercial interests in any products described in the manuscript.

Reprint requests to James A. Sharpe, MD, Division of Neurology, University Health Network–Toronto Western Hospital, EC 5-042, 399 Bathurst Street, Toronto, Ontario, Canada M5T 2S8.

ISSN 0161-6420/00/$–see front matter
PII S0161-6420(99)00092-5

perimetry was performed by one of the authors (JAS). Patients were seated 1 m away from a 2-m^2 black target screen in a well-lit room. A spotlight directed from above and slightly to one side was used for additional illumination. Fixation was adjusted for height by raising or lowering the patients' chair. Patients wore spectacle correction (if they had any refractive error) and were instructed to fixate on a 1-cm white fixation target at the center of the screen. One eye was covered. Using a 3-mm diameter white test object mounted on a black wand, the field, about 10 degrees to either side of the vertical and horizontal meridians was explored by moving the test object at a rate of 2 to 3 degrees per second from the periphery toward the center. Any point of disappearance or reappearance was marked with a black-headed pin. When a defect was identified, its margins were determined by moving the test object centrifugally from the defective to the seeing area. The defect was further confirmed by rotating the wand 180 degrees to make the test object appear or disappear at the same location. The density of the defect was assessed by asking the patient whether he or she could see larger white objects or could count fingers or detect any hand or finger movement in the area of field loss. The blind spot was tested to ensure patients' reliability. The fellow eye was tested in the same manner.

Goldmann and Humphrey perimetry were performed by any one of three experienced technicians in our unit, using similar methods described previously.[6–9] For Goldmann kinetic perimetry, patients were seated before the perimeter with the nontested eye occluded. The patient's refraction (with additional diopters adjusted for age) was placed in a lens holder and refined with plus or minus spheres. The machine was calibrated (according to the manufacturer's instructions) and the background-to-target luminosity ratio was set at 1:33. The blind spot was mapped out using a I2e or I4e test object to ensure patient reliability. Relative defects in the visual field were then mapped out using three standard objects (V4e, I4e, and I2e), with additional isopters plotted as indicated. To mark the peripheral edge of an isopter, the test object was brought in (at a rate of 2 to 3 degrees per second) from the far periphery toward fixation until it was seen. For scotoma testing, a test object was presented inside the region of field loss and moved radially in a straight line until it was seen. Because the central 2 degrees (which corresponds to the opening of the telescope for eye position monitoring) could not be tested with the Goldmann perimeter with the patient looking at a central fixating target, tests of macular sparing were performed similar to scotoma testing but with the fixating target displaced 5 degrees horizontally or vertically. The fellow eye was then tested.

The central 30-2 threshold program was used for Humphrey perimetry in all but one patient (patient 3), who was tested with the central 24-2 program. All patients were tested with a white, size III (4 mm^2) stimulus against a background illumination of 31.5 asb, with the other test parameters set at their default values (fixation target—central; blind spot check size—III; test speed—normal). Patient information, including age, date of test, corrective lens used (based on distance prescription with age-appropriate convex spherical add), pupil diameter, and visual acuity, were entered into the machine. Patients' fixation and position were checked every 1 to 2 minutes in the video eye monitor, with adjustments made as necessary.

A field was considered unreliable on tangent screen or Goldmann perimetry if the blind spot could not be plotted or if the examiner assessed the patient's fixation to be too poor to plot an adequate field. A field on Humphrey perimetry was considered unreliable if the blind spot was not plotted. We did not consider "fixation losses," "false positives," or "false negatives" in this determination because of a lack of specific guidelines[5] and because a test that meets the manufacturer's criteria for unreliability may still be clinically useful.[9] Patients with unreliable fields on any one of the three perimetric examinations were excluded from the study.

Because of the inherent differences in perimetric techniques and instrumentation, variables such as test distance, object size, and background illumination could not be completely controlled for. Therefore, visual field examinations were performed with parameters that are standard in clinical practice: 3-mm test object at a distance of 1 m for tangent screen examination, V4e, I4e, and I2e test objects at a distance of 300 mm for Goldmann perimetry, and size III (4 mm^2) test object at a test distance of 333 mm for Humphrey perimetry. For comparison, results obtained from Goldmann I4e and I2e, rather than V4e, isopters were used because the I4e and I2e test objects are more sensitive than V4e to detect field loss in the central 30 degrees of vision, which corresponds to the area of field tested by tangent screen and the 30-2 program of Humphrey perimetry. In addition, we defined visual field results as corresponding to one another if the discrepancy between different perimetric techniques was $\leq$5 degrees. We selected this 5-degree discrepancy threshold to compensate for the lack of control over these variables and also to account for the fact that the test points measured by the Humphrey central 30-2 program are separated from one another by 6 degrees. In addition to the gray scale, we also used the numeric, total deviation, and pattern deviation plots to interpret visual field results from Humphrey perimetry.

The visual field results from the three perimetric techniques were compared with one another and were then compared with MR images to determine their accuracy in detecting and localizing lesions in patients with occipital lobe infarcts.

Results

Twelve patients had reliable fields in all three perimetric examinations and well-defined occipital infarcts on MRI and were included in the analysis. There were nine men and three women, with a mean age of 57.5 years (range, 29–80 years). The mean duration of patients' symptoms of impaired vision was 8 months (range, 4–20 months). The results of visual field examinations using tangent screen, Goldmann, and Humphrey perimetry are shown in Figure 1.

Table 1 summarizes our interpretation of the visual field abnormalities in each patient on the basis of results from tangent screen examination, Goldmann, and Humphrey perimetry. All three perimetric techniques revealed homonymous field defects that respected the vertical meridian and detected the presence of postchiasmal lesions in all 12 patients.

Table 2 summarizes the location of lesions predicted by each of the three perimetric techniques and compares them with the actual location of lesions on MRI. In all 12 patients, visual fields obtained from tangent screen and Goldmann perimetry agreed with each other (i.e., discrepancy $\leq$ 5 degrees) and corresponded well with the location of lesions on MRI. However, in five patients (patients 3, 6, 7, 9, and 11), visual fields from Humphrey perimetry did not correspond with those from tangent screen and Goldmann perimetry (i.e., discrepancy $>$ 5 degrees) or to lesions located on MRI.

Humphrey perimetry showed incongruous homonymous field defects, inaccurately localizing lesions to the optic tract, lateral geniculate nucleus, or proximal optic radiation in two patients (patients 3 and 7). For example, in patient 7, tangent screen and Goldmann perimetry detected a left inferior congruous homonymous central scotoma (Fig 1), suggesting a lesion in the right superior striate cortex. Humphrey perimetry, on the other hand, detected a left incongruous homonymous hemianopia (Fig 1), suggesting damage to a proximal part of the postchiasmal pathway. The actual lesion was found to be in the right superior occipital pole and distal optic radiation on MRI (Fig 2), corresponding to

that suggested by tangent screen and Goldmann perimetry but not Humphrey perimetry. Similar findings were observed in patient 3.

Tangent screen and Goldmann perimetry detected sparing of the macula in nine patients, who were found to have sparing of the posterior occipital cortex or occipital pole on MRI. The central 30-2 program of Humphrey perimetry, however, failed to detect macular sparing in three of these nine patients (patients 6, 9, and 11). Similarly, in patient 3, tangent screen detected sparing of the central 5 degrees and Goldmann perimetry detected sparing of the central 6 degrees of vision, whereas the central 24-2 program of Humphrey perimetry found no macular sparing (Fig 1). On MRI, the actual lesion was found to spare the occipital pole (Fig 3), corresponding to the field suggested by tangent screen and Goldmann perimetry.

To further assess the ability of Humphrey perimetry to detect macular sparing in those patients who had macular sparing on kinetic perimetry, but undetected by the central 30-2 Humphrey program (or by the central 24-2 program in patient 3), we performed central 10-2 and macula threshold tests on patients 3, 6, and 11 (patient 9 was lost to follow-up). In patient 3, the central 10-2 threshold program revealed sparing of the central 2 degrees in the right eye, but no macular sparing in the left eye, as shown in the total and pattern deviation plots (Fig 4). The macula threshold test, however, detected sparing of the central 2 degrees of vision in both eyes (Fig 4). Similar testing with the central 10-2 program revealed macular sparing in patients 6 and 11 (Fig 5).

The extent of visual field loss was overestimated by Humphrey perimetry in one patient (patient 11). In patient 11, both tangent screen and Goldmann perimetry revealed a right congruous homonymous superior quadrantanopia (Fig 1), suggesting a lesion in the left inferior occipital cortex. Humphrey perimetry, however, revealed a right congruous incomplete homonymous hemianopia involving the upper and lower field but denser superiorly than inferiorly (Fig 1), suggesting a lesion either in the optic radiation of the left temporal lobe or in the left occipital cortex involving both the superior and inferior calcarine cortex. On MRI, the lesion was found to be limited to the left inferior occipital cortex, with no involvement superiorly (Fig 6), in agreement with the site predicted by tangent screen and by Goldmann perimetry.

Discussion

With the advent of newer generations of automated perimeters and the availability of more sophisticated software programs, such as STATPAC of the Humphrey Field Analyzer, automated perimetry is increasingly relied on for detection and localization of visual pathway damage in clinical practice. Establishing its ability to detect abnormal fields and its accuracy to localize lesions is important for the diagnosis and management of neurologic diseases. Prior studies have shown that automated suprathreshold static perimetry (e.g., Fieldmaster)[4,10] and threshold static perimetry (e.g., Octopus, Humphrey)[5,11] were comparable to manual kinetic perimetry (e.g., Goldmann) in detecting visual field abnormalities in neurologic diseases. McCrary and Feigon,[11] for example, found that the Octopus perimeter (using threshold static strategy) detected visual field defects almost identical to those found on the Goldmann perimeter in 21 (84%) of the 25 patients studied. Similarly, Beck et al[5] found that visual fields obtained from Humphrey perimetry (using the central 30-2 threshold program) were similar or differed only slightly from those from Goldmann perimetry in 60 (87%) of the 69 eyes studied.

Those studies[4,5,10,11] used older generation perimeters without software programs that are now available. For example, early models of Humphrey Field Analyzer did not have advanced software programs such as STATPAC that compare a patient's visual field data with age-corrected normals (total deviation and the corresponding probability plots), correct a patient's visual field data for diffuse loss (pattern deviation and the corresponding probability plots), or calculate global indices that summarize a patient's data. In addition, those studies[4,5,10,11] evaluated the ability of automated static perimetry to *detect* visual field loss by comparing them with Goldmann perimetry, but they did not assess the accuracy of automated static perimetry to *localize* lesions by correlating visual field findings with high-resolution imaging.

Precise localization of lesions by careful perimetry is clinically important because accurate pre-imaging localization aids physicians in selecting the most appropriate neuroimaging technique and in focusing on a specific area in question. In addition, perimetric localization of lesions has substantial value in determining whether the pattern of a patient's visual field defect is adequately accounted for by imaging. This study systematically evaluated and compared the accuracy of manual kinetic (using a tangent screen and the Goldmann perimeter) and automated static perimetry (the Humphrey Field Analyzer) in detecting and localizing lesions by correlating them with MR images in patients with occipital infarcts.

Comparison of Different Perimetric Techniques

Because of differences in static versus kinetic perimetric methods and variables such as targets used, testing distance, and background illumination, the information obtained from different perimetric methods was quite distinct. Exact correspondence of the fields obtained from the three methods would not be expected. However, the question we addressed in this study was, given different perimetric techniques used in clinical practice, does one or another of them provide the most precise information about the presence and location of lesions? We therefore performed the three perimetric examinations according to standard practice and used MRI findings as the independent variable to assess the accuracy of each method in detecting and localizing lesions.

We found that all three perimetric techniques *detected* the presence of postchiasmal lesions. However, *localization* of lesions differed with different techniques. Visual fields obtained from tangent screen and Goldmann perimetry were concordant and corresponded well with lesions location on MR images in all 12 patients. Visual fields from the central 30-2 program of Humphrey perimetry did not correspond to those from tangent screen, Goldmann perimetry, or MRI in five patients (patients 3, 6, 7, 9, and 11); it inaccurately localized the lesion to the proximal part of the postchiasmal pathway by revealing incongruous fields in two patients (patients 3 and 7), failed to detect sparing of the posterior occipital cortex or occipital pole in four patients (patients 3, 6, 9, and 11), and estimated a larger extent of damage in one patient (patient 11) when compared with MR images and manual kinetic perimetry.

Patient 1

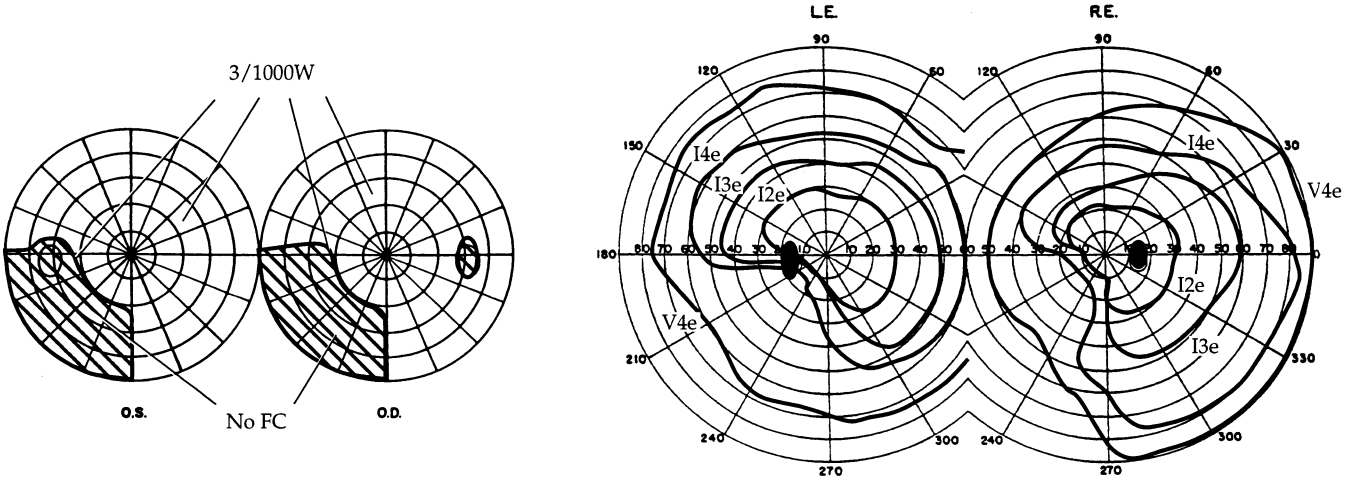

Patient 2

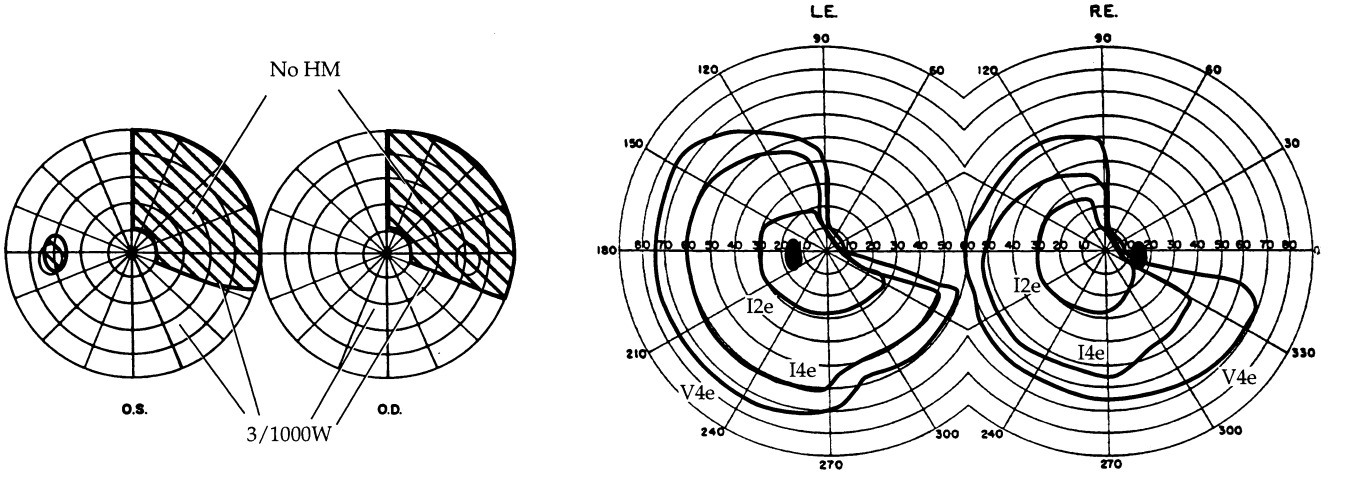

Patient 3

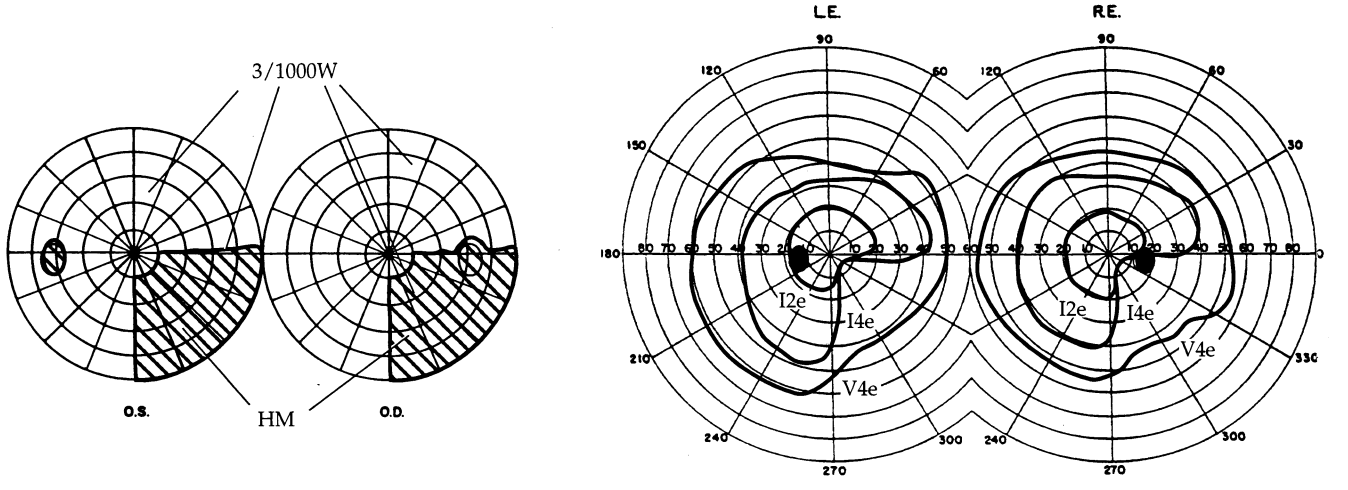

Figure 1. Results of visual field examinations using tangent screen, Goldmann, and Humphrey perimetries. (3/1000W = 3-mm diameter white object at a test distance of 1 m; FC = finger counting; FS = finger seen; HM = hand motion) (**Figure 1** *continues*)

Patient 1 (continued)

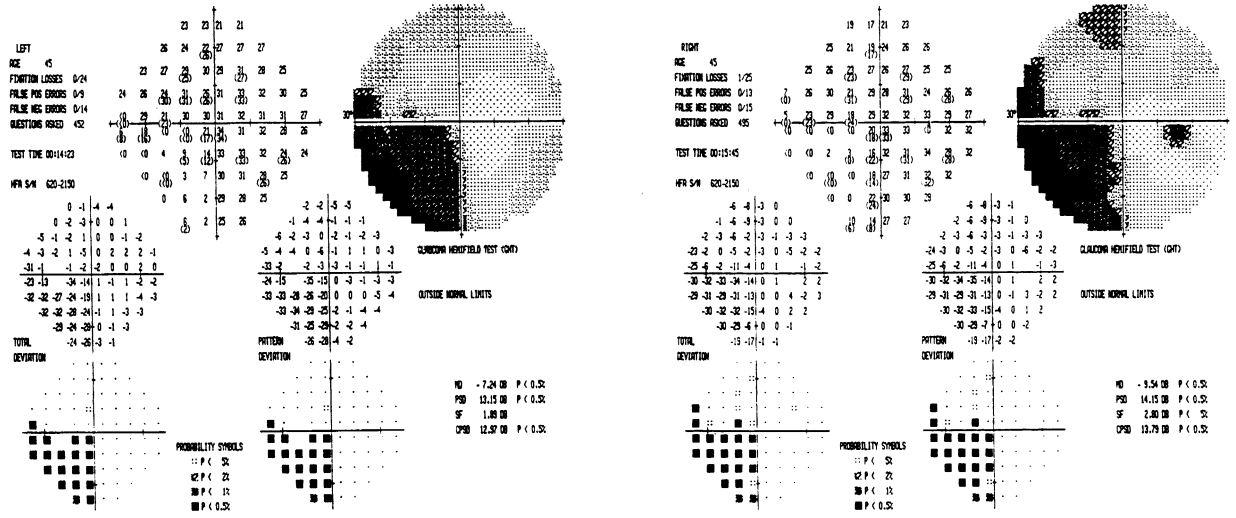

Patient 2 (continued)

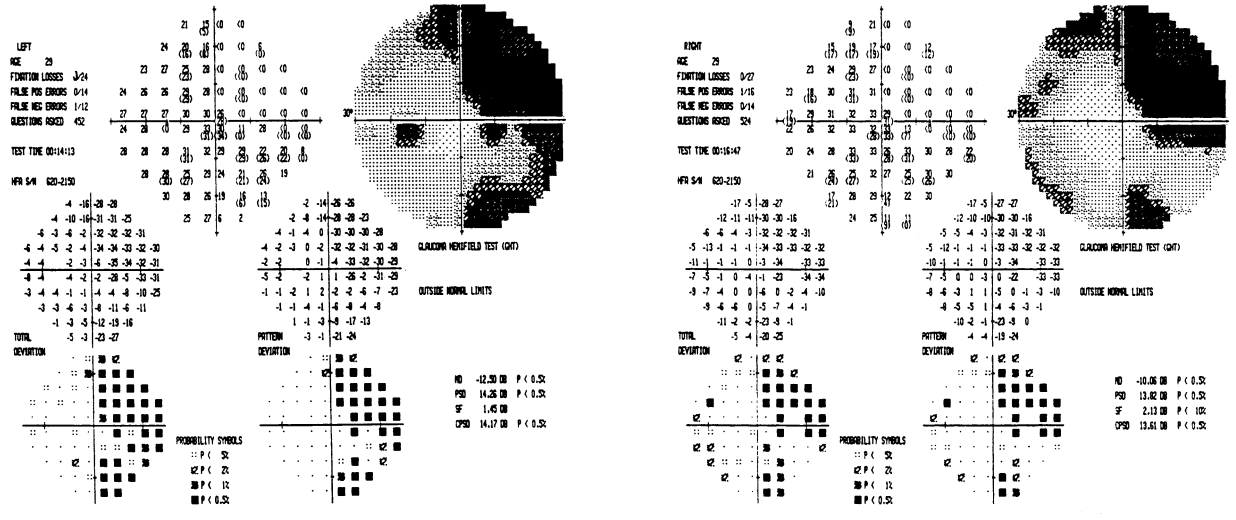

Patient 3 (continued)

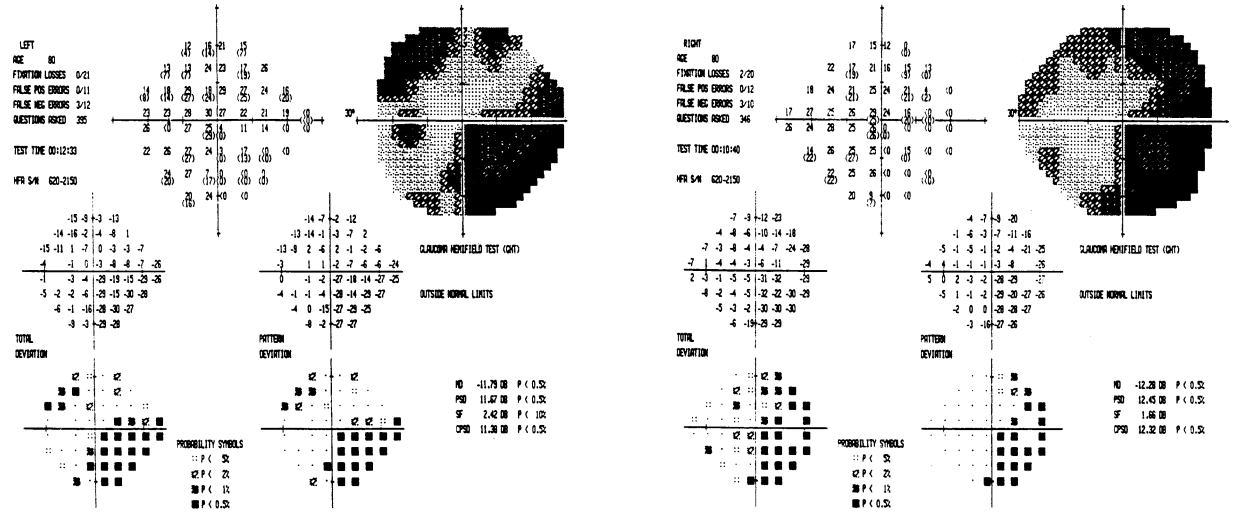

(**Figure 1** *continued*)

Patient 4

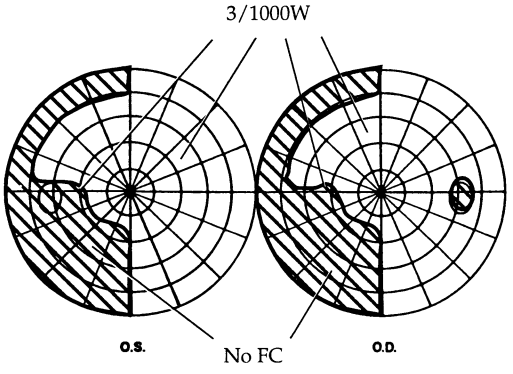

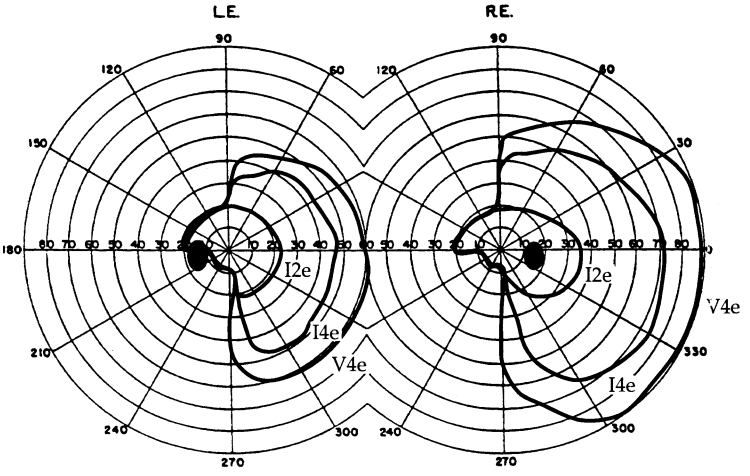

Patient 5

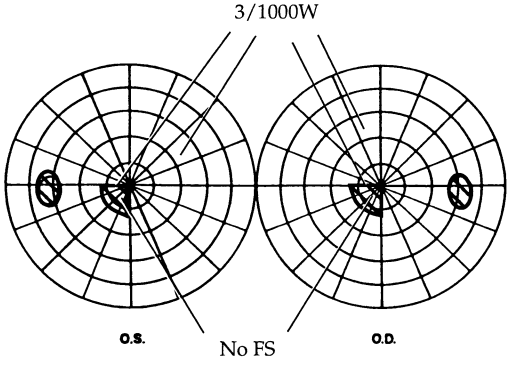

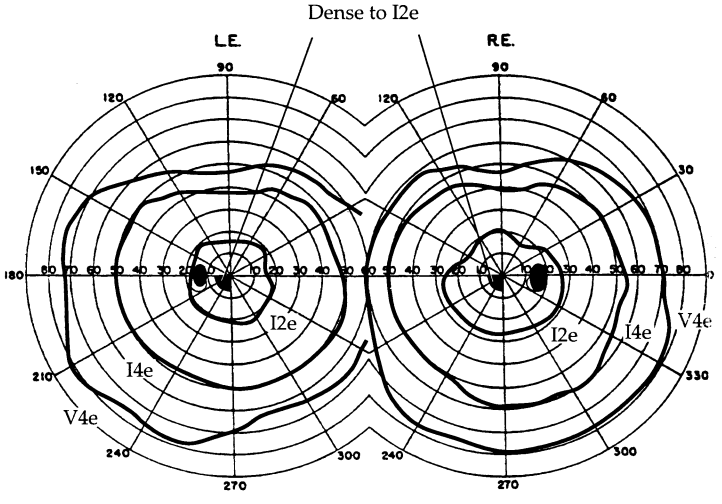

Patient 6

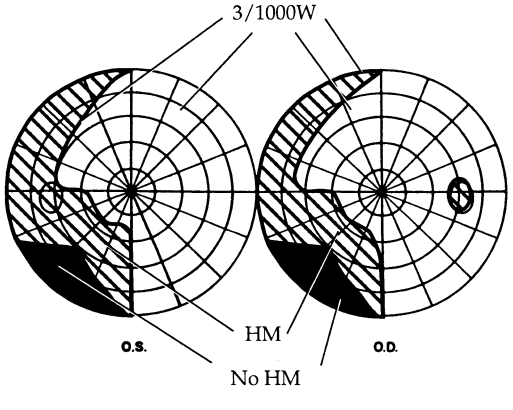

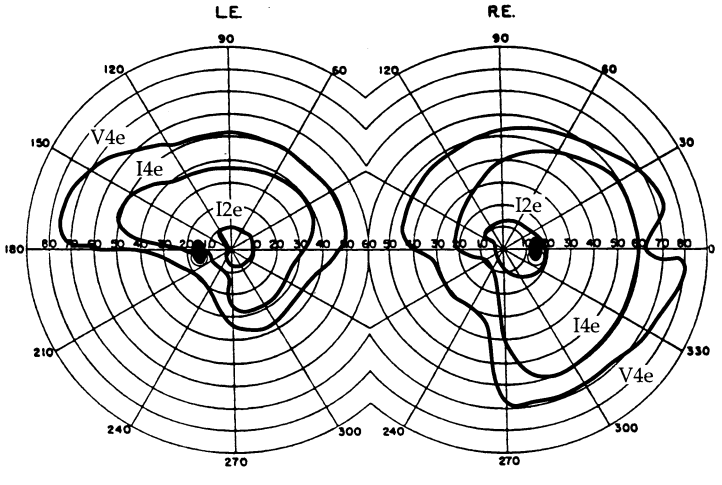

(**Figure 1** *continued*)

Patient 4 (continued)

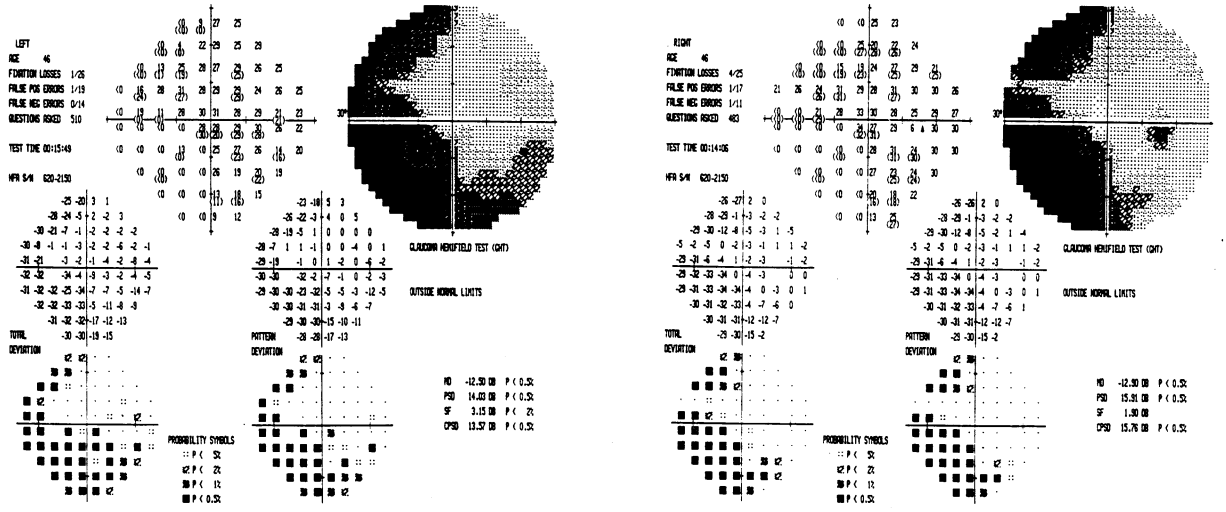

Patient 5 (continued)

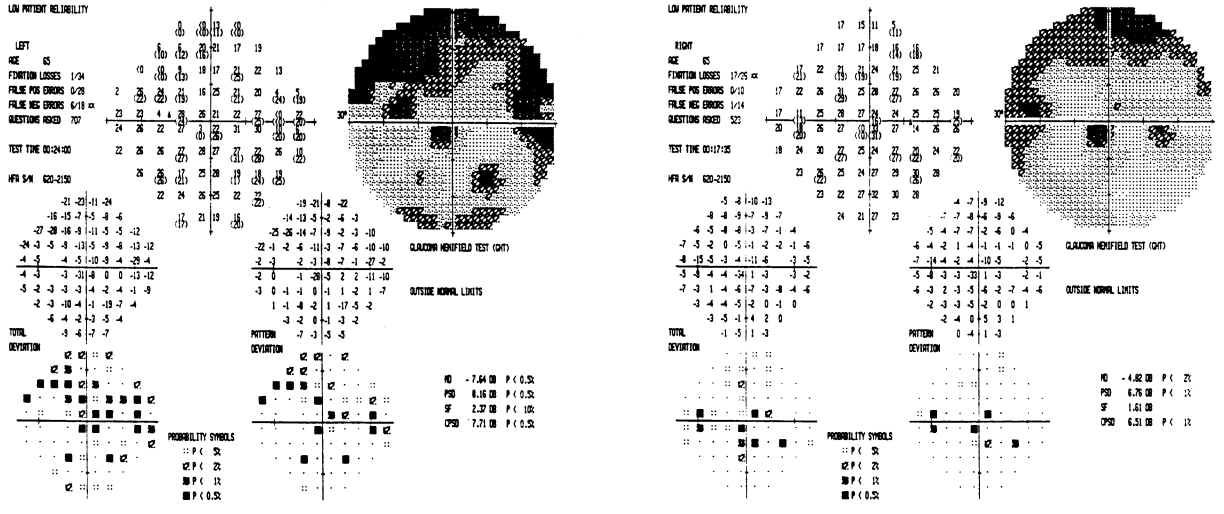

Patient 6 (continued)

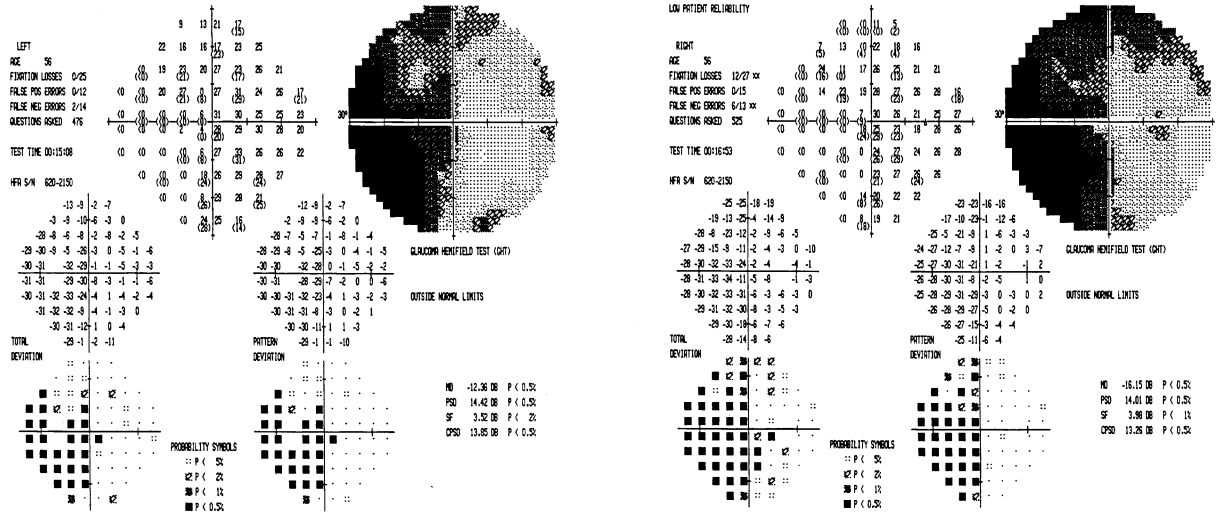

(**Figure 1** *continued*)

Patient 7

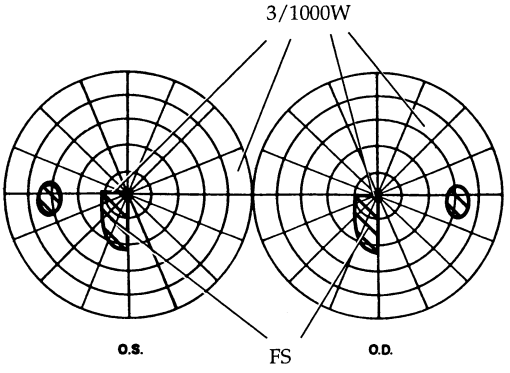

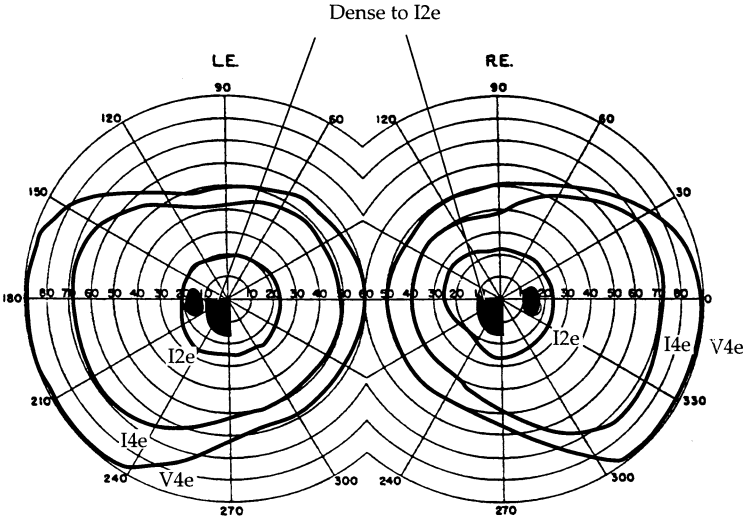

Patient 8

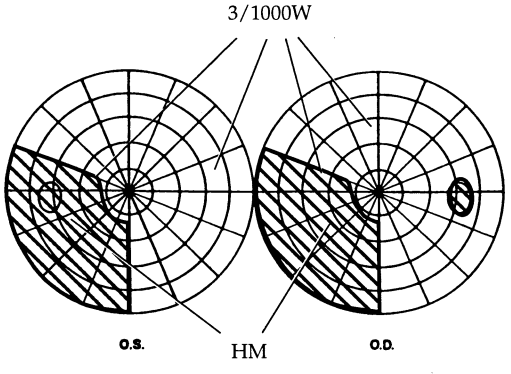

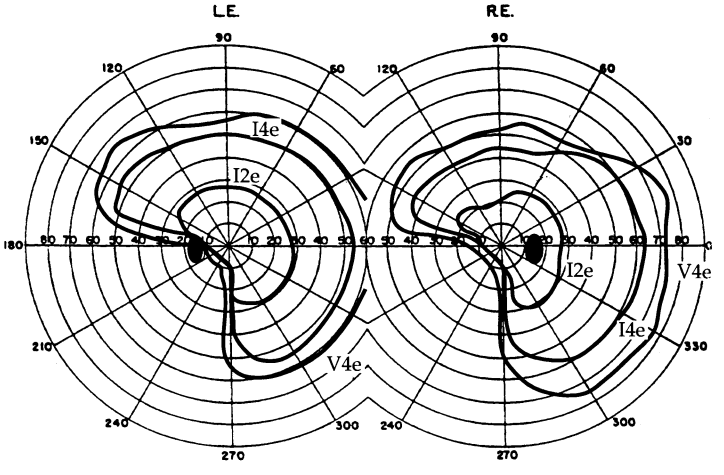

Patient 9

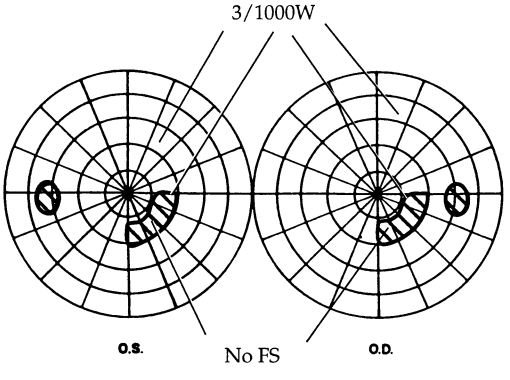

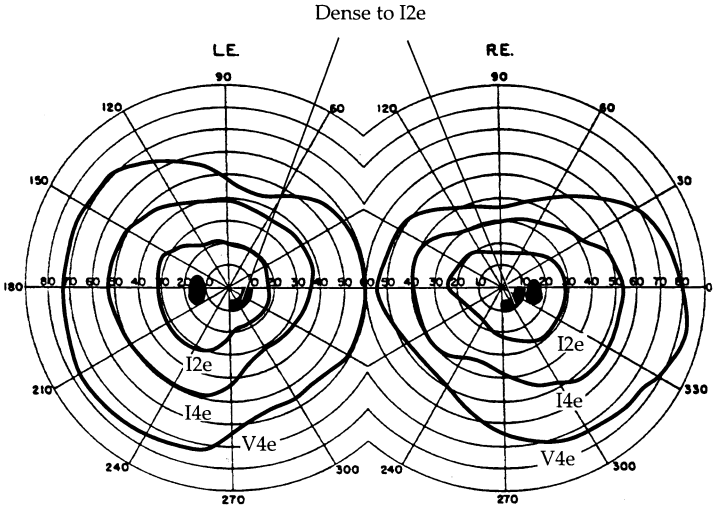

(**Figure 1** *continued*)

Patient 7 **(continued)**

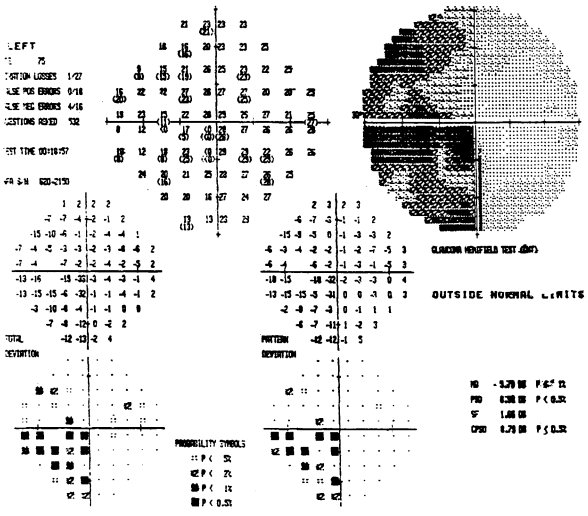

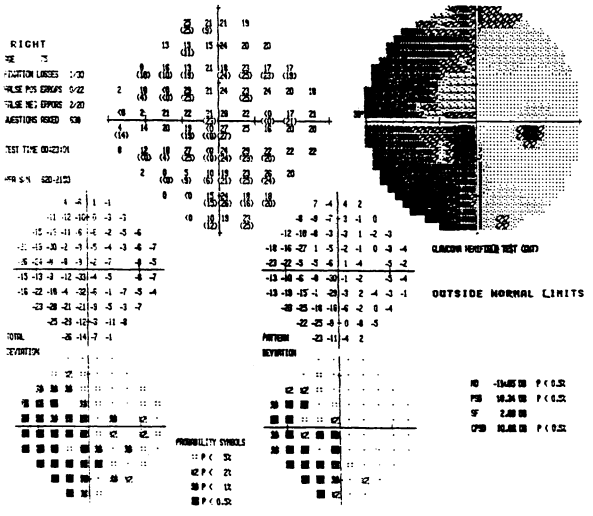

Patient 8 **(continued)**

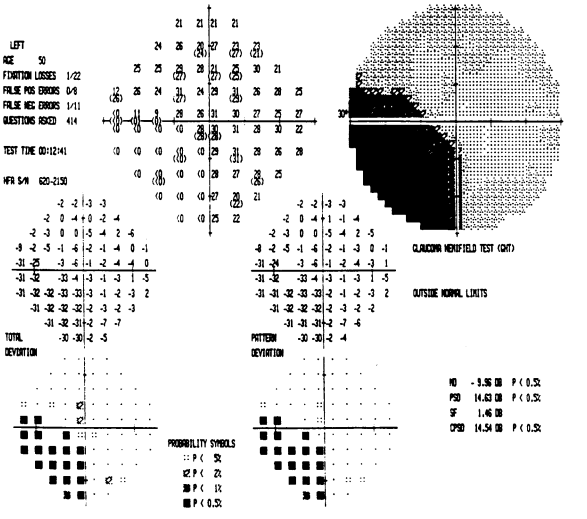

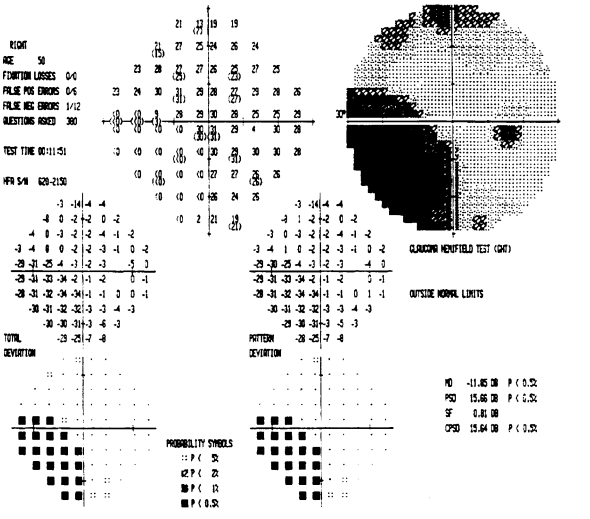

Patient 9 **(continued)**

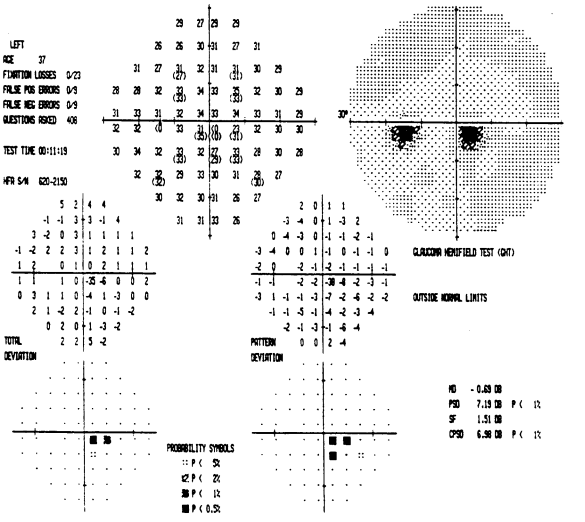

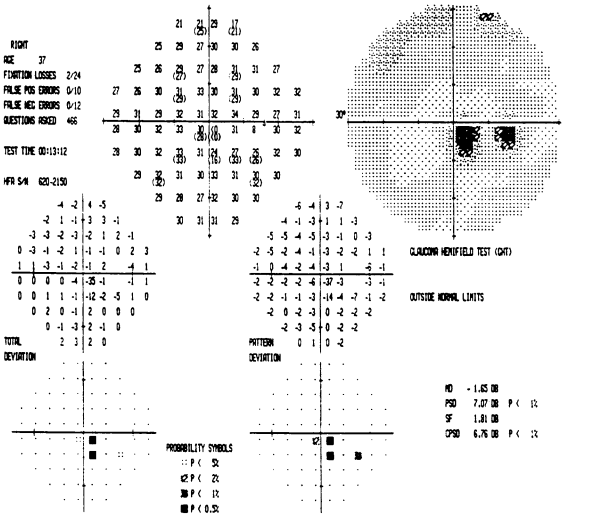

(**Figure 1** *continued*)

Patient 10

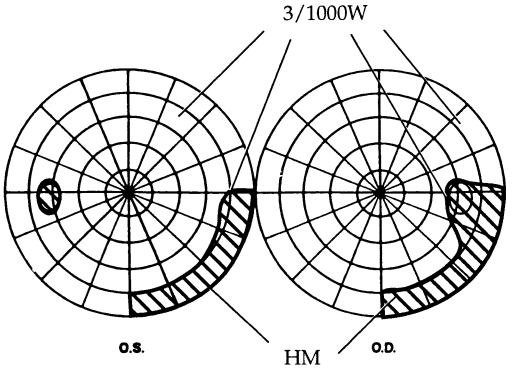

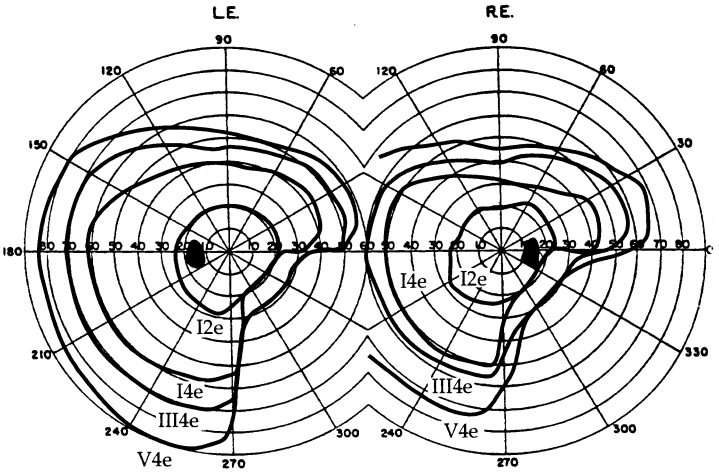

Patient 11

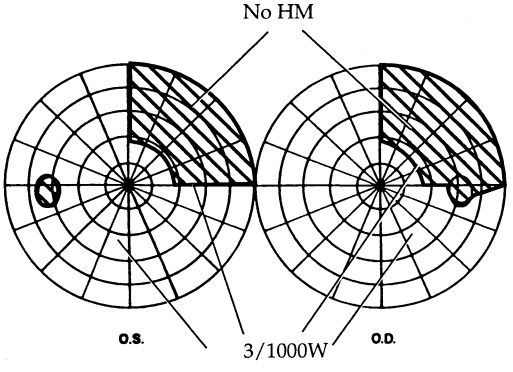

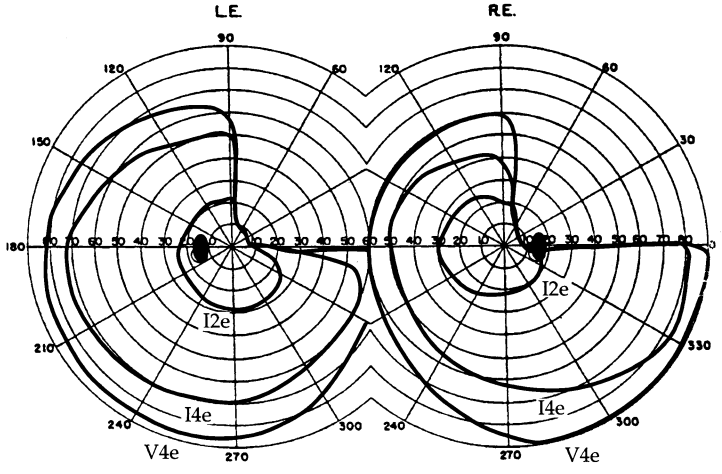

Patient 12

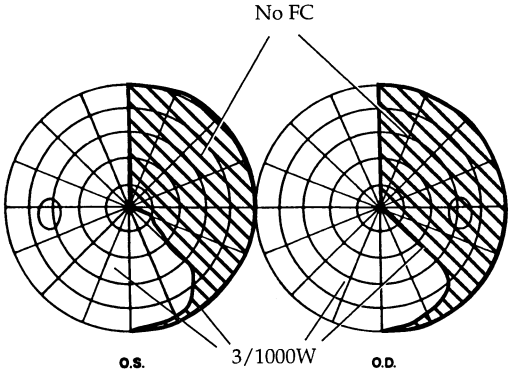

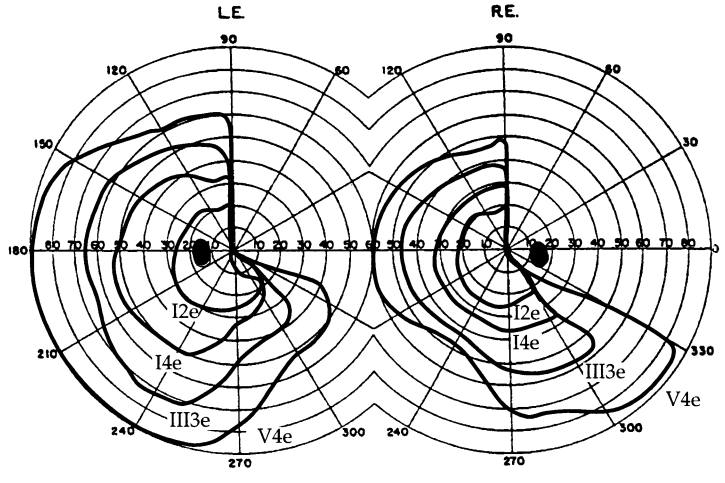

(**Figure 1** *continued*)

Patient 10 (continued)

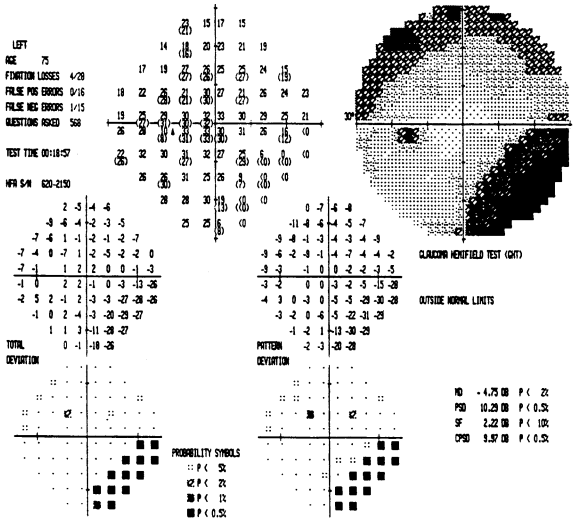

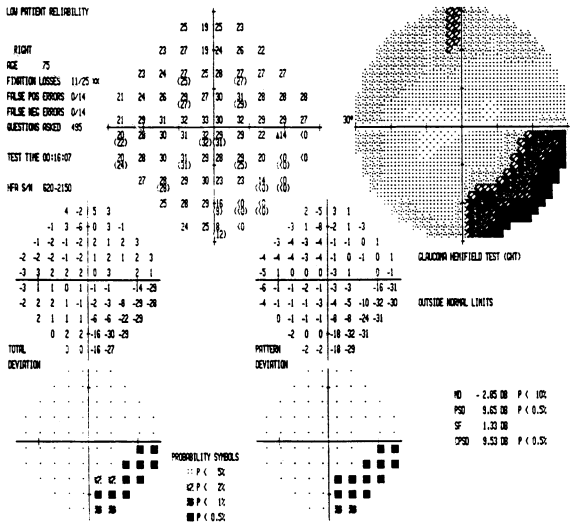

Patient 11 (continued)

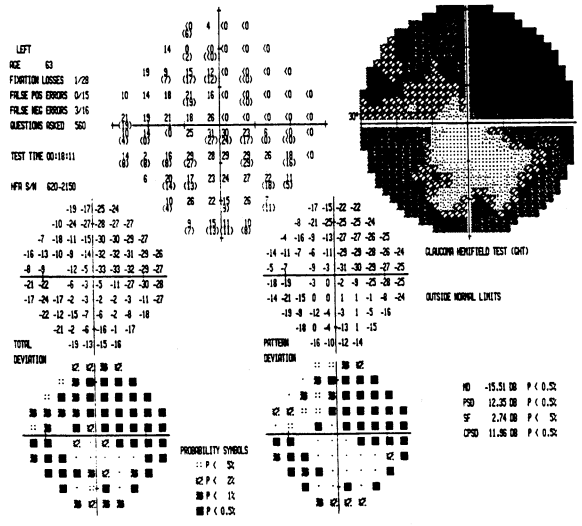

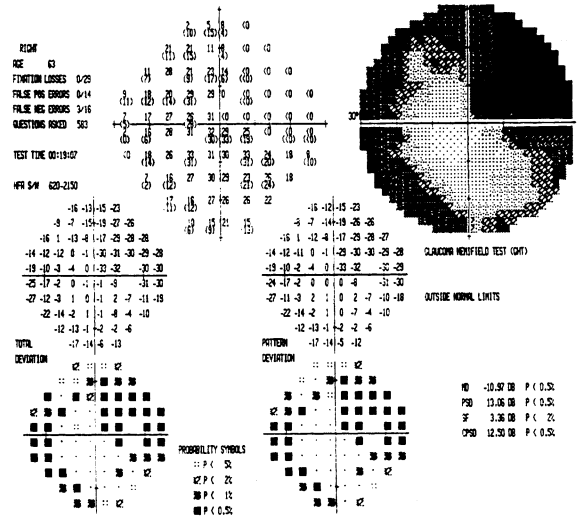

Patient 12 (continued)

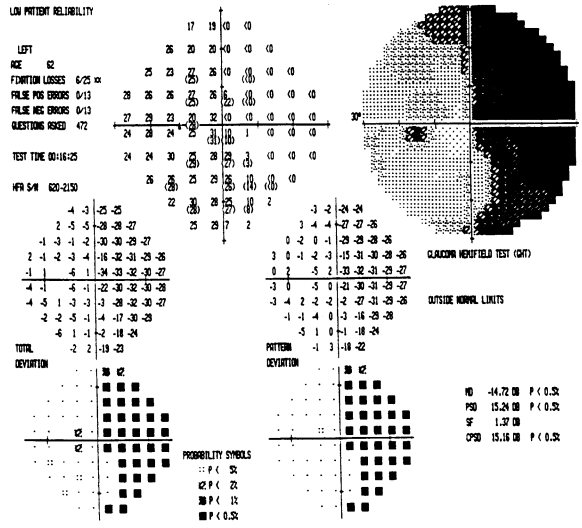

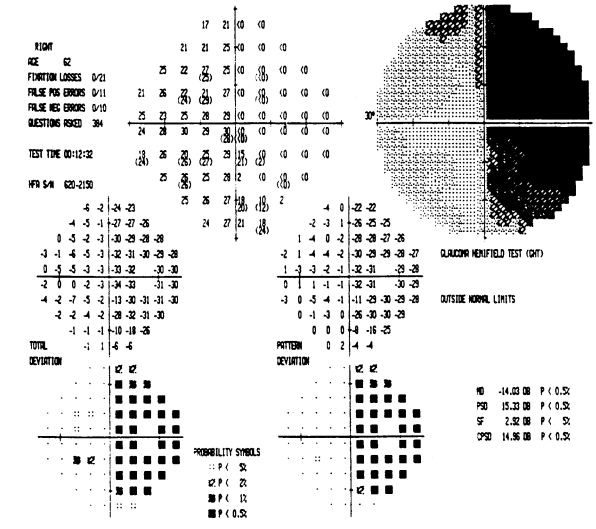

(**Figure 1** *continued*)

Table 1. Interpretations of Visual Field Results from Tangent Screen, Goldmann, and Humphrey Perimetries

Patient	Tangent Screen	Goldmann Perimetry	Humphrey (Central 30-2)
1	L inf congruous homonymous quadrantanopia (from 180 to 270 meridian); spared central 11°	L inf congruous homonymous quadrantanopia (from 180 to 270 meridian); constricted field on V4e; spared central 15°, 9°, and 8° on I4e, I3e and I2e, respectively	Reliable test Gray tone: L inf congruous homonymous quadrantanopia; spared central 3° PD (prob): no sparing of central fixation
2	R congruous incomplete homonymous hemianopia (from 330 to 90 meridian); spared central 5°	R congruous incomplete homonymous hemianopia (from 345 to 90 meridian); spared central 8°, 6°, and 5° on V4e, I4e, and I2e, respectively	Reliable test Gray tone and PD (prob): R congruous incomplete homonymous hemianopia (denser sup than inf); spared central 5°
3	R inf congruous homonymous quadrantanopia (from 270 to 0 meridian); spared central 5°	R inf congruous homonymous incomplete quadrantanopia (from 270 to 0 meridian); spared central 45°, 6°, and 6° on V4e, I4e, and I2e, respectively	Reliable test Gray tone and PD (prob): R incongruous incomplete homonymous hemianopia (denser inf than sup); no sparing of central fixation
4	L congruous incomplete homonymous hemianopia (from 90 to 270 meridian); spared central 20° from 90 to 180 meridian; spared central 8° from 180 to 270 meridian	L congruous incomplete homonymous hemianopia (from 90 to 270 meridian); spared central 20° from 90 to 180 meridian; spared central 8° from 180 to 270 meridian on all tested stimuli	Reliable test Gray tone and PD (prob): L congruous incomplete homonymous hemianopia (denser inf than sup); spared central 15° superiorly and central 5° inferiorly
5	L inf congruous homonymous central scotoma (from 180 to 270 meridian); involved central 0 to 6°	L inf congruous homonymous central scotoma (from 180 to 270 meridian); involved central 0 to 6° on all tested stimuli	High fixation loss but otherwise reliable with normal SF rate OD; high false-negative rate but otherwise reliable OS Gray tone and PD (prob): L inf congruous homonymous central scotoma from 0 to 6°
6	L congruous incomplete homonymous hemianopia; spared central 15° from 135 to 180 meridian; spared central 9° from 180 to 270 meridian	L congruous incomplete homonymous hemianopia (from 120 to 270 meridian); spared central 20°, 10°, and 3° on V4e, I4e, and I2e, respectively	Reliable test Gray tone and PD (prob): L congruous incomplete homonymous hemianopia; no sparing of central fixation
7	L inf congruous homonymous central scotoma (from 180 to 270 meridian); extending from 0 to 6° at the horizontal meridian, and from 0 to 12° at the vertical meridian	L inf congruous homonymous central scotoma (from 180 to 270 meridian); extending from 0 to 10° at the horizontal meridian, and from 0 to 15° at vertical meridian on I4e and I2e	Reliable test Gray tone and PD (prob): L incongruous incomplete homonymous hemianopia (denser inf than sup); involved central 0 to 30°
8	L congruous incomplete homonymous hemianopia (from 165 to 270 meridian); spared central 6°	L congruous incomplete homonymous hemianopia (from 165 to 270 meridian); spared central 10°, 7°, and 7° on V4e, I4e, and I2e, respectively	Reliable test Gray tone and PD (prob): L congruous incomplete homonymous hemianopia (denser inf than sup), spared central 6°
9	R inf congruous homonymous paracentral scotoma (from 270 to 0 meridian); involved central 6 to 10°	R inf congruous homonymous paracentral scotoma (from 270 to 345 meridian); involved central 6 to 10° on all tested stimuli	Reliable test Gray tone and PD (prob): R inf congruous homonymous paracentral scotoma from 0 to 8°
10	R congruous incomplete homonymous inf quadrantanopia (from 270 to 0 meridian); spared central 20°	R congruous incomplete homonymous inf quadrantanopia (from 270 to 0 meridian); spared central 30° on V4e and III3e; spared central 20° on I4e and I2e	High fixation loss but otherwise reliable with normal SF rate OD; reliable test OS Gray tone and PD (prob): R congruous incomplete homonymous inf quadrantanopia; spared central 17°
11	R congruous homonymous sup quadrantanopia (from 0 to 90 meridian); spared central 9°	R congruous homonymous sup quadrantanopia (from 0 to 90 meridian); spared central 9° on all tested stimuli	Reliable test Gray tone and PD (prob): R congruous incomplete homonymous hemianopia (denser sup than inf); no sparing of central fixation
12	R congruous incomplete homonymous hemianopia (from 315 to 90 meridian); no sparing of central fixation	R congruous incomplete homonymous hemianopia (from 330 to 90 meridian on V4e; from 315 to 90 meridian on III3e, I4e, and I2e); no sparing of central fixation	Reliable test OD; high fixation loss but otherwise reliable with normal SF rate OS Gray tone and PD (prob): R congruous incomplete homonymous hemianopia, sparing of part of inf field along 270 meridian; no sparing of central fixation

inf = inferior; L = left; OD = right eye; OS = left eye; PD (prob) = pattern deviation (probability plot); R = right; SF rate = short tem fluctuation rate; sup = superior.

Patient Reliability

Although the lack of agreement of visual field findings between Humphrey perimetry and tangent screen examination, Goldmann perimetry, or MRI might be related to patients' test reliability, our results indicate that this was not the case. During tangent screen examination and Goldmann perimetry, the examiner could interact continuously with

Table 2. Lesion Localization Using Tangent Screen, Goldmann, and Humphrey Perimetries and Actual Lesion Locations on MRI

Patient	Predicted Lesions Location Using			Actual Lesion Location on MRI
	Tangent Screen	*Goldmann*	*Humphrey*	
1	R striate cortex; spared occipital pole	R striate cortex; spared occipital pole	R striate cortex; spared occipital pole	R striate cortex; spared occipital pole
2	L striate cortex; spared occipital pole	L striate cortex; spared occipital pole	L striate cortex; spared occipital pole	L striate cortex; spared occipital pole
3	L striate cortex; spared occipital pole	L striate cortex; spared occipital pole	L substriate lesion (incongruous field)	L striate cortex and optic radiation; spared occipital pole
4	R striate cortex; spared occipital pole	R striate cortex; spared occipital pole	R striate cortex; spared occipital pole	R striate cortex; spared occipital pole
5	R superior striate cortex; involved occipital pole	R superior striate cortex; involved occipital pole	R superior striate cortex; involved occipital pole	R superior striate cortex; involved occipital pole
6	R striate cortex; spared occipital pole	R striate cortex; spared occipital pole	R striate cortex; involved occipital pole	R striate cortex; spared occipital pole
7	R superior striate cortex; involved occipital pole	R superior striate cortex; involved occipital pole	R substriate lesion (incongruous field)	R superior striate cortex and optic radiation; involved occipital pole
8	R striate cortex; spared occipital pole	R striate cortex; spared occipital pole	R striate cortex; spared occipital pole	R striate cortex; spared occipital pole
9	L superior striate cortex; spared occipital pole	L superior striate cortex; spared occipital pole	L superior striate cortex; involved occipital pole	L superior striate cortex; spared occipital pole
10	L superior striate cortex; spared posterior cortex	L superior striate cortex; spared posterior cortex	L superior striate cortex; spared posterior cortex	L superior striate cortex; spared posterior cortex
11	L inferior striate cortex; spared occipital pole	L inferior striate cortex; spared occipital pole	L striate cortex; involved occipital pole	L inferior striate cortex; spared occipital pole
12	R striate cortex; involved occipital pole	R striate cortex; involved occipital pole	R striate cortex; involved occipital pole	R striate cortex; involved occipital pole

L = left; R = right; substriate lesion = lesion in the proximal portion of the postchiasmal pathway.

patients and assess their reliability. With Humphrey perimetry, the test program automatically determined fixation loss, false-positive and false-negative rates, and indicated the field as having "low patient reliability" when any one of these "reliability parameters" met the manufacturer's criteria for unreliability. In this study, three patients (patients 5, 10, and 12) were designated as "unreliable" by Humphrey perimetry. Patient 5 had a high fixation loss and false-negative rate, whereas patients 10 and 12 had high rates of fixation loss. We interpreted their fields as reliable and included them in the study because their other "reliability parameters" were normal and they all had low short-term fluctuation rates. Nonetheless, inclusion of these three patients in our analysis could *not* explain the discrepant results among different perimetric techniques; all three of them had Humphrey field results that were concordant with those from tangent screen and Goldmann perimetry. Conversely, of the five patients (patients 3, 6, 7, 9, and 11) who were found to have discrepant results among different visual field techniques, none had "low patient reliability"on Humphrey perimetry.

Detection of Macular Sparing

Establishing the presence and extent of macular sparing is pertinent because it specifies an occipital lobe lesion and indicates the amount of central vision that a patient possesses. Because the central 2 degrees could not be tested with the Goldmann perimeter with the patient looking at a central fixating target, we tested macular sparing by displacing the fixation target 5 degrees horizontally or vertically. With this technique, we found that both tangent screen and Goldmann perimetry accurately detected macular sparing in each of the nine patients who were shown to have sparing of the posterior mesial occipital cortex and occipital pole on MRI.

The central 30-2 threshold program of Humphrey perimetry, on the other hand, failed to detect macular sparing in three patients (patients 6, 9, and 11). This is explained by the program: although the gray tone printout gives the impression that every point is tested, the central 30-2 program measures only the threshold values at 76 predetermined points that are separated from each other by 6 degrees and are offset from the horizontal and vertical meridians by 3 degrees. For example, adjacent to the horizontal meridian, the tested points lie at approximately 2, 8, 14, 20, and 26 degrees, so the program does not provide threshold information at approximately 3 to 7, 9 to 13, 15 to 19, 21 to 25, and 27 to 30 degrees. Therefore, small field defects and macular sparing may not show up in the gray tone, numeric, total, or pattern deviation plots printout.

The central 10-2 program of Humphrey perimetry measures the threshold values at 68 predetermined points that are separated from each other by 2 degrees, and, therefore, should be better able to detect small field defects in the central 10 degree of vision. Using the central 10-2 program, further testing was performed on three of the four patients (patients 3, 6, and 11) who were found to have no macular sparing with the central 30-2 or 24-2 program (one of the four patients, patient 9, was not available for follow-up

Figure 2. Axial T2-weighted MR image of patient 7 showing an infarct in the right occipital cortex.

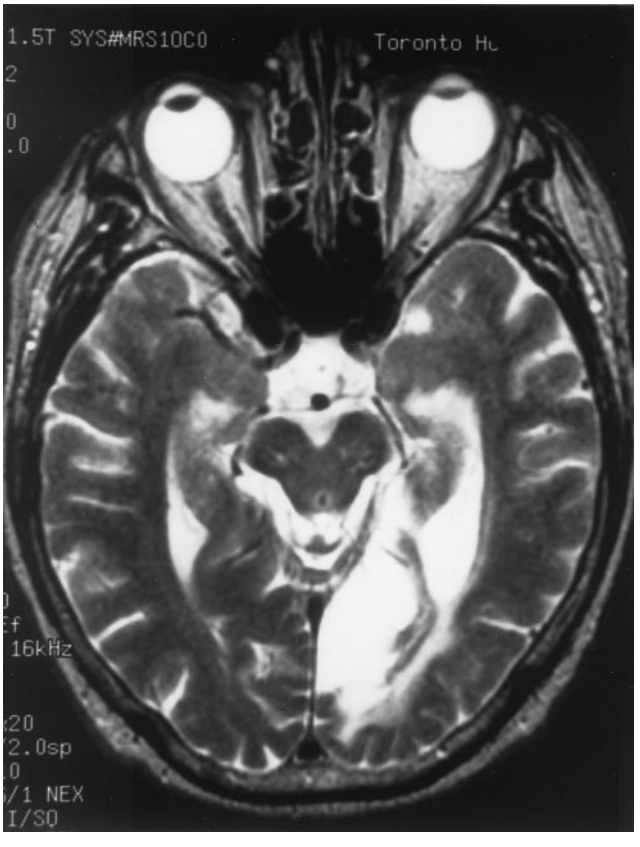

Figure 3. Axial T2-weighted MR image of patient 3 showing an infarct in the left mesial occipital cortex, with sparing of the occipital pole.

testing with the central 10-2 program). We found that the central 10-2 program detected macular sparing, and the extent of sparing was concordant with results from tangent screen and Goldmann perimetry in all three patients tested. Our results indicate that the flexibility of tangent screen and Goldmann perimetry allow the examiner to tailor his or her testing strategy, such that a small field defect can be detected and explored in a single test session. To detect macular sparing with Humphrey perimetry, additional testing using the central 10-2 threshold program or the macula threshold test may be required to obtain comparable information to that from tangent screen or Goldmann perimetry.

Localization of Lesions

Fibers from corresponding fields of each eye are separated in the anterior portion of the postchiasmal pathway. Although controversies exist,[12–22] rostral lesions of the postchiasmal pathway are generally considered to produce incongruous homonymous hemianopias, notably if they involve the optic tract or lateral geniculate nucleus, whereas more posterior lesions involving the optic radiation or striate cortex cause congruous defects. We found that in two patients (patients 3 and 7), none of the visual field techniques alone was able to predict the full extent of the imaged lesion. Tangent screen and Goldmann examinations detected congruous homonymous field defects and predicted occipital lesions, whereas Humphrey perimetry revealed incongruous homonymous field defects that suggested damage to the proximal part of the postchiasmal pathway. MR imaging on these two patients, however, revealed occipital lobe lesions that involved the distal optic radiation. Perimetric effects of damage at different sites along the optic radiation has not been correlated with modern brain imaging. Because damage to the distal optic radiation is not known to cause incongruous field loss,[12–22] our findings indicate that tangent screen and Goldmann perimetry provide more precise information about the congruity of field defects and, hence, the location of lesions than does Humphrey perimetry. Alternatively, our findings by static perimetry signify that lesions of the distal optic radiation might cause genuine incongruity that is not detected by kinetic perimetry. Further investigations correlating the results of automated static perimetry with MRI loci of optic radiation damage are warranted.

Extent of Visual Field Defects and Lesions Size

The extent of field defect detected by Humphrey perimetry was greater than those suggested by tangent screen and Goldmann perimetry in three patients (patients 3, 7, and 11). This may be related to the phenomenon of statokinetic dissociation, whereby patients perceive moving but not stable objects.[23,24] Statokinetic dissociation would make the margins of field loss detected by Humphrey (static) perimetry larger than the margins of field loss detected by kinetic perimetry. Thus, Humphrey perimetry might be expected to detect lesions that kinetic perimetry does not, but in our 12 patients, we found kinetic perimetry to be equally sensitive for detection.

Patient 3

Central 10-2 Threshold Test

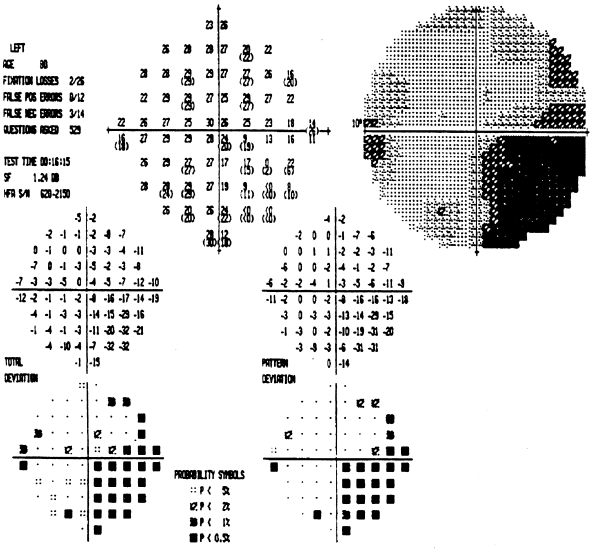

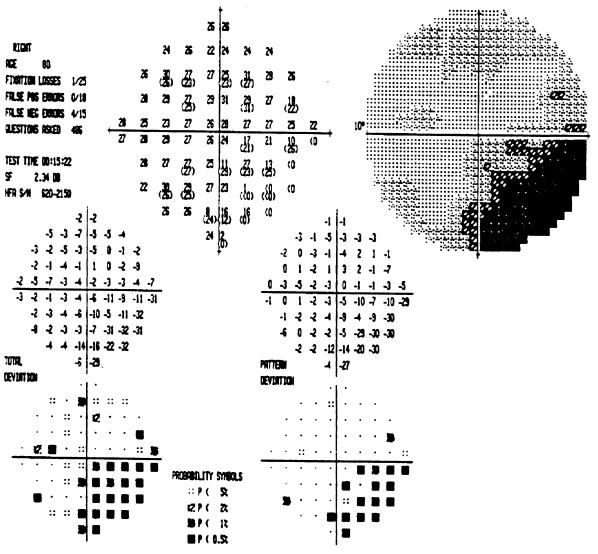

Macula Threshold Test

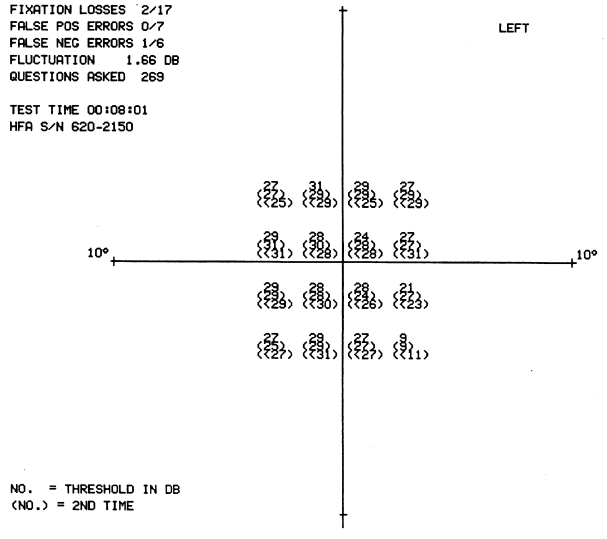

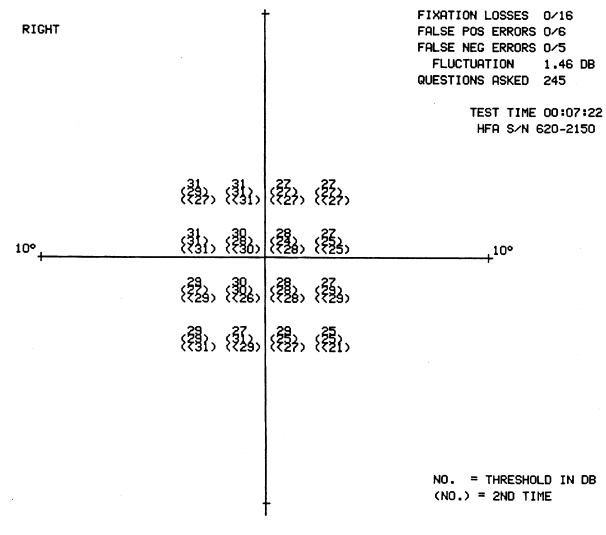

Figure 4. Results of additional visual field testing using Humphrey perimetry in patient 3. Central 10-2 program revealed sparing of the central 2 degrees in the right eye but no macular sparing in the left eye. Macula threshold test, however, detected sparing of the central 2 degrees of vision in both eyes.

In addition, recent studies on cortical plasticity in adult cats and monkeys showed that deactivation or an altered pattern of activation can result in topographic reorganization in the primary visual cortex[25] by mechanisms such as reshaping the receptive field of cortical cells[26,27] and increasing the sensitivity of deprived cells in the visual cortex.[28] Although cortical rearrangement after lesions in the visual pathways cannot restore function to the destroyed tissue,[29] it may help to compensate for gaps in perception by "filling-in" of visual field defects.[25,28,30] By measuring the threshold values of individual points rather than plotting the isopters of the three-dimensional "hill of vision," static perimetry may be more sensitive than kinetic perimetry to "unmask" the filling-in process of cortical adaptation and hence reveal a more extensive visual field loss.

Static perimetry also detected a larger area of visual field

Patient 6

Central 10-2 Threshold Test

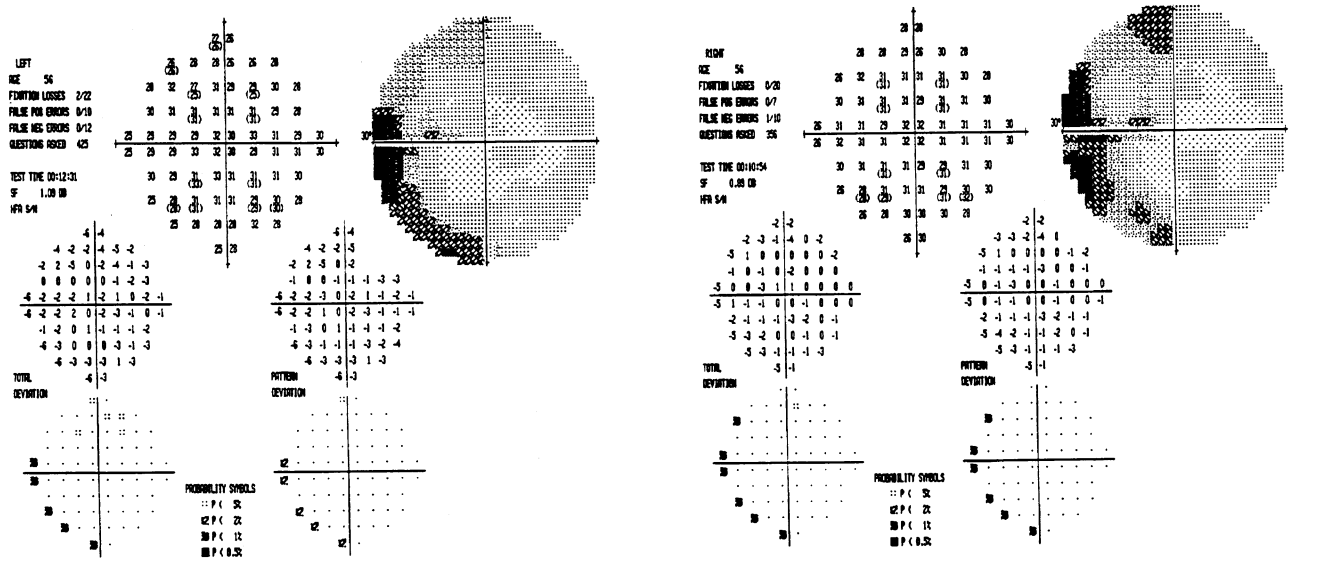

Patient 11

Central 10-2 Threshold Test

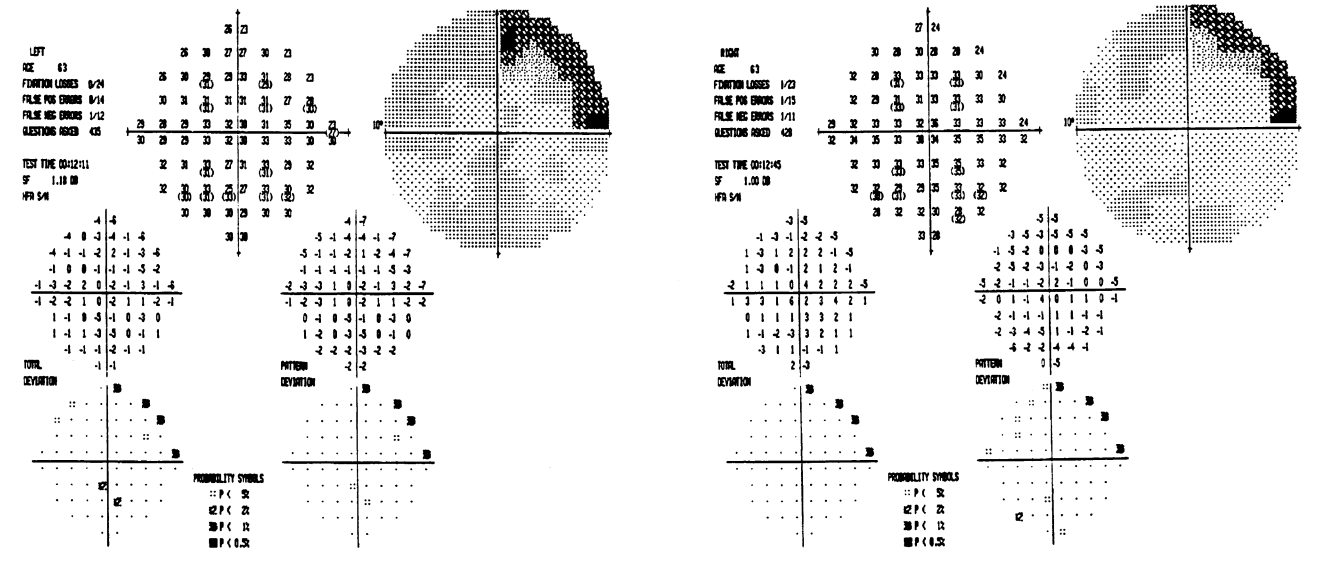

Figure 5. The central 10-2 program of Humphrey perimetry detected macular sparing in two other patients (patients 6 and 11), who were found to have no macular sparing with the central 30-2 program.

loss than that suggested by MRI in one patient (patient 11). The MRI was performed 7 months after the patient's initial presentation when edema and any ischemic penumbra should have completely resolved, so that the area of signal change represents an area of brain necrosis not transient or fluctuating loss of neuronal function. The larger area of field loss detected by static perimetry suggests either that static perimetry misrepresents the genuine anatomic extent of damage to the visual pathway or that static perimetry is more sensitive than MRI in detecting incomplete loss of a population of neurons. In patient 11, however, Humphrey perimetry implicated a lesion involving the upper bank of

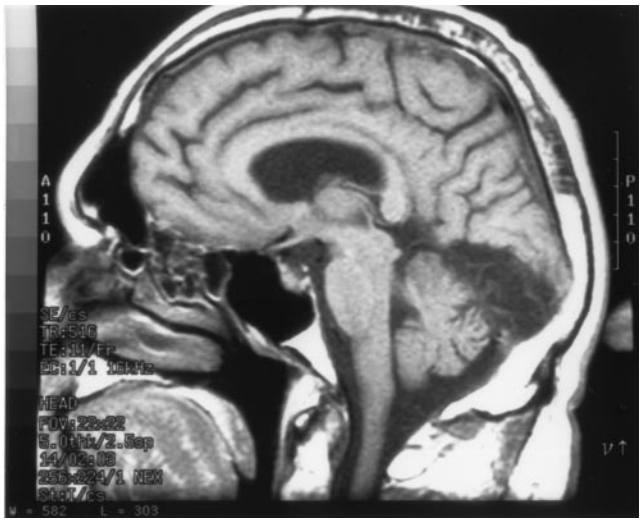

Figure 6. Sagittal T1-weighted MR image of patient 11 showing an infarct in the left inferior occipital cortex, with no involvement of the cortex superiorly.

the calcarine fissure as well as the lower bank, contrary to the MRI finding of an infarct confined below the calcarine fissure.

Alternate Modern Perimetric Techniques

Other perimetric tests designed to target specific visual mechanisms may prove to be more sensitive than conventional manual or kinetic perimetry to detect visual field loss and might better represent the genuine location and extent of lesions in the visual pathway.[31–34] For example, using Short Wavelength Automated Perimetry (SWAP), Keltner and Johnson[31] found that SWAP detected visual field loss in patients with neuro-ophthalmologic disorders who have an otherwise normal visual field on conventional automated perimetry. In cases in which visual field loss was evident on conventional automated perimetry, SWAP detected larger areas of impaired visual field.[31]

In addition, newer threshold strategies, such as SITA Standard and SITA Fast, of Humphrey Field Analyzer II reduce the mean testing time by 50% to 70% compared with the standard full-threshold test.[35–37] Decreased testing time reduces the effect of fatigue on patients and may improve the precision of Humphrey perimetry in localizing cerebral lesions

Conclusion

The results of this investigation indicate that both manual kinetic perimetry (tangent screen and the Goldmann perimeter) and automated static perimetry (Humphrey Field Analyzer) are satisfactory as screening tests to detect occipital lesions. However, tangent screen and Goldmann perimetry provide information about the location and extent of lesions as identified by MRI that is most consistent with prevailing knowledge[12–22] of the perimetric effects of lesions in the postgeniculate visual pathway.

References

1. Katz J, Tielsch JM, Quigley HA, Sommer A. Automated perimetry detects visual field loss before manual Goldmann perimetry. Ophthalmology 1995;102:21–6.
2. Trope GE, Britton R. A comparison of Goldmann and Humphrey automated perimetry in patients with glaucoma. Br J Ophthalmol 1987;71:489–93.
3. Schmied U. Automated (Octopus) and manual (Goldmann) perimetry in glaucoma. Albrecht von Graefes Arch Exp Ophthalmol 1980;213:239–44.
4. Keltner JL, Johnson CA. Automated and manual perimetry—a six-year overview. Special emphasis on neuro-ophthalmic problems. Ophthalmology 1983;91:68–85.
5. Beck RW, Bergstrom TJ, Lichter PR. A clinical comparison of visual field testing with a new automated perimeter, the Humphrey Field Analyzer, and the Goldmann perimeter. Ophthalmology 1985;92:77–82.
6. Tate GW Jr, Lynn JR. Principles of Quantitative Perimetry: Testing and Interpreting the Visual Field. New York: Grune & Stratton, Inc., 1977;130–44, 152–78.
7. Harrington DO, Drake MV. The Visual Fields: Text and Atlas of Clinical Perimetry, 6th ed. St. Louis: Mosby, 1990.
8. Humphrey Field Analyzer Operator's Manual. San Leandro, CA: Allergan Humphrey, 1987; Section 3:1–36.
9. Choplin NT, Edwards RP. Visual Field Testing with the Humphrey Field Analyzer. Thorofare, NJ: SLACK Inc, 1995.
10. Johnson CA, Keltner JL, Balestrery FG. Suprathreshold static perimetry in glaucoma and other optic nerve disease. Ophthalmology 1979;86:1278–86.
11. McCrary JA III , Feigon J. Computerized perimetry in neuro-ophthalmology. Ophthalmology 1979;86:1287–301.
12. Spalding JMK. Wounds of the visual pathway. Part II: The striate cortex. J Neurol Neurosurg Psychiatry 1952;15:169–83.
13. Marino R Jr, Rasmussen T. Visual field changes after temporal lobectomy in man. Neurology 1968;18:825–35.
14. Van Buren JM, Baldwin M. The architecture of the optic radiation in the temporal lobe of man. Brain 1958;81:15–40.
15. Falconer MA, Wilson JL. Visual field changes following anterior temporal lobectomy: their significance in relation to "Meyer's loop" of the optic radiation. Brain 1958;81:1–14.
16. Harrington DO. Visual field character in temporal and occipital lobe lesions. Arch Ophthalmol 1961;66:778–92.
17. Harrington DO. Localizing value of incongruity in defects in the visual fields. Arch Ophthalmol 1939;21:453–64.
18. McAuley DL, Russell RWR. Correlation of CAT scan and visual field defects in vascular lesions of the posterior visual pathways. J Neurol Neurosurg Psychiatry 1979;42:298–311.
19. Koerner F, Teuber HL. Visual field defects after missile injuries to the geniculo-striate pathway in man. Exp Brain Res 1973;18:88–113.
20. Shacklett DE, O'Connor PS, Dorwart RH, et al. Congruous and incongruous sectoral visual field defects with lesions of the lateral geniculate nucleus. Am J Ophthalmol 1984;98:283–90.
21. Luco C, Hoppe A, Schweitzer M, et al. Visual field defects in vascular lesions of the lateral geniculate body. J Neurol Neurosurg Psychiatry 1992;55:12–15.
22. Kölmel HW. Homonymous paracentral scotomas. J Neurol 1987;235:22–5.
23. Riddoch G. Dissociation of visual perception due to occipital injuries with special reference to appreciation of movement. Brain 1917;40:15–57.
24. Safran AB, Glaser JS. Statokinetic dissociation in lesions of

the anterior visual pathways; a reappraisal of the Riddoch phenomenon. Arch Ophthalmol 1980;98:291–5.
25. Kaas JH. Neurobiology. How cortex reorganizes. Nature 1995;375:735–6.
26. Gilbert CD, Wiesel TN. Receptive field dynamics in adult primary visual cortex. Nature 1992;356:150–2.
27. Pettet MW, Gilbert CD. Dynamic changes in receptive-field size in cat primary visual cortex. Proc Natl Acad Sci USA 1992;89:8366–70.
28. Darian-Smith C, Gilbert CD. Topographic reorganization in the striate cortex of the adult cat and monkey is cortically mediated. J Neurosci 1995;15:1631–47.
29. Safran AB, Landis T. Plasticity in the adult visual cortex: implications for the diagnosis of visual field defects and visual rehabilitation. Curr Opin Ophthalmol 1996;7:53–64.
30. Gilbert CD. Plasticity in visual perception and physiology. Curr Opin Neurobiol 1996;6:269–74.
31. Keltner JL, Johnson CA. Short-wavelength automated perimetry in neuro-ophthalmologic disorders. Arch Ophthalmol 1995;113:475–81.
32. Lindblom B, Hoyt WF. High-pass resolution perimetry in neuro-ophthalmology. Clinical impressions. Ophthalmology 1992;99:700–5.
33. Wall M, Montgomery EB. Using motion perimetry to detect visual field defects in patients with idiopathic intracranial hypertension. A comparison with conventional automated perimetry. Neurology 1995;45:1169–75.
34. Johnson CA, Samuels SJ. Screening for glaucomatous visual field loss with frequency-doubling perimetry. Invest Ophthalmol Vis Sci 1997;38:413–25.
35. Bengtsson B, Olsson J, Heijl A, Rootzen H. A new generation of algorithms for computerized threshold perimetry, SITA. Acta Ophthalmol Scand 1997;75:368–75.
36. Bengtsson B, Heijl A, Olsson J. Evaluation of a new threshold visual field strategy, SITA, in normal subjects. Swedish Interactive Thresholding Algorithm. Acta Ophthalmol Scand 1998; 76:165–9.
37. Nordmann JP, Brion F, Hamard P, Mouton-Chopin D. Evaluation des programmes périmétriques Humphrey SITA Standard et SITA Fast chez les patients normaux et glaucomateus [Eng. abstr.]. J Fr Ophtalmol 1998;21:549–54.